Wide-area Measurements-based Two-level Control Design Considering Power System Operation Uncertainties

Murilo E. C. Bento
University of Sao Paulo
Sao Carlos, SP, Brazil
murilo.bento@usp.br

Daniel Dotta
University of Campinas
Campinas, SP, Brazil
dottad@unicamp.br

Rodrigo A. Ramos
University of Sao Paulo
Sao Carlos, SP, Brazil
rodrigo.ramos@ieee.org

***Abstract*—In this paper, a procedure to design Wide-Area Damping Controller based on the solution of the Riccati equation considering uncertainties of the system operation is proposed. Originally, the method based on Riccati equation does not consider uncertainties, providing a satisfactory damping only for the nominal operating condition. In this paper, the resulting controller presents fixed order, communication time-delays and it is robust to load, topological variations and time-delays. Besides, the closed-loop system presents quadratic stability. The performance of the proposal procedure is evaluated through the modal analysis and non-linear time-domain simulations of the Brazilian 7 bus Equivalent Power System Model, an IEEE benchmark system for small-signal analysis.**

***Index Terms*—Small-Signal Stability, Wide-Area Damping Control, Wide-Area Measurement Systems, System Uncertainties.**

I. Introduction

Poorly damped or unstable oscillation modes are an important concern in Small-Signal Stability because they limit the power flow between areas as well as may cause power system blackouts [1]. Traditionally, this problem has been successfully tackled by the use of local controllers at the generators. However, even well setting local controllers may present limited performance under topological and load variation for real-time operating conditions [2].

In recent years, the expansion of wide-area measurement systems (WAMS) has provided attractive control strategies in order to minimize the influence of these low-damping oscillations [3]–[15]. Among several control structures considered for wide-area damping control (WADC), the two-level control structure presents potential interest in the literature for power system application [16]. The two-level control structure presents local controllers and a central controller. The local controllers, corresponding to the well-known automatic voltage regulator - power system stabilizer (AVR-PSS) at the generators, ensure a satisfactory performance. The central controller ensures the optimization of the global system performance or stabilizes the power system in situations where topological variations or load changes require the re-tuning of the local control. The main central controller advantage is to coordinate the low-level controller in order to improve system-wide performance. Notice that, in this work, despite the local control is part of the two-level controller, the two controllers are not designed simultaneously. The local control is considered already well adjusted by the local utility and coordinated changes will involve utility agreement which is not suitable for real-time operation.

There is not a standard method for WADC design. In the literature, the main methods proposed for WADC design are: linear-quadratic design (where a Riccati equation is solved) [3], [4], Linear Matrix Inequalities (LMIs) [4]–[6], Genetic Algorithms [7]–[12] and Swarm Intelligence [13]–[15]. The great advantage of methods based on solution of Riccati equation is that it can be solved even for large-scale systems [3]. However, the proposed method did not include operating uncertainties in the control design method. As a result, the controller may not be effective in providing satisfactory damping for uncertainties, such as topological and load variations, find out during power system operation.

The main contributions of this paper is the application of the method based on the solution of the Riccati equation considering power system operating uncertainties [17]. The resulting centralized controller presents fixed and low-order compared with the power system size. The controller is also robust to load, topological and time-delays variations. Comparing with the previous approach, presented in [3], this method will reduce the necessity of the central controller retuning because it considers operating uncertainties in the control design moment. Modal analysis and non-linear time-domain simulations are performed for the design validation and performance assessment in the multimachine Southern/Southeastern Brazilian equivalent power system.

The paper is organized as follows: section II presents the power system modeling, the time delay model and control structure; section III present the proposed procedure based on Riccati equation considering operating uncertainties; section IV evaluates through modal analysis and non-linear time-domain simulation the resulting controllers of the original and

This work was supported by Fundação de Amparo à Pesquisa do Estado de São Paulo (FAPESP) under grants no. 2015/02569-6, 2015/18806-7 and 2015/24245-8

proposed procedure; section V presents the conclusions.

II. System Model

A. Power System Modeling

The power system model is linearized around a nominal operating point and it is defined by [1]:

$$\dot{\mathbf{x}} = \mathbf{A}\mathbf{x} + \mathbf{B}\mathbf{u} \tag{1}$$

$$\mathbf{y} = \mathbf{C}\mathbf{x} \tag{2}$$

where $\mathbf{x}$, $\mathbf{u}$ and $\mathbf{y}$ are the state, input and output vectors respectively.

B. Time Delay Model

A second order Padé approximation [18] is used to represent the time delay model. Its transfer function is

$$\mathbf{G_d}(s) = \frac{6 - 2Ts}{6 + 4Ts + (sT)^2} \tag{3}$$

where T is the time delay. The state space equations are

$$\dot{\mathbf{x}}_\mathbf{d} = \mathbf{A_d}\mathbf{x_d} + \mathbf{B_d}\mathbf{u_d} \tag{4}$$

$$\mathbf{y_d} = \mathbf{C_d}\mathbf{x_d} + \mathbf{D_d}\mathbf{u_d} \tag{5}$$

where $\mathbf{x_d}$ is the delay state vector, $\mathbf{u_d}$ is the input vector, $\mathbf{y_d}$ is the output vector and

$$\mathbf{A_d} = \begin{bmatrix} 0 & -\frac{6}{T^2} \\ 1 & -\frac{4}{T} \end{bmatrix} \quad \mathbf{B_d} = \begin{bmatrix} \frac{6}{T^2} \\ -\frac{2}{T} \end{bmatrix} \tag{6}$$

$$\mathbf{C_d} = \begin{bmatrix} 0 & 1 \end{bmatrix} \quad \mathbf{D_d} = \begin{bmatrix} 0 \end{bmatrix} \tag{7}$$

Defining $\bar{\mathbf{x}} = \begin{bmatrix} \mathbf{x} & \mathbf{x_i} & \mathbf{x_i} \end{bmatrix}$ where subscripts $\mathbf{i}$ and $\mathbf{o}$ denote the input and the output delays respectively, the state space system is given by

$$\dot{\bar{\mathbf{x}}} = \bar{\mathbf{A}}\bar{\mathbf{x}} + \bar{\mathbf{B}}\mathbf{u_{di}} \tag{8}$$

$$\mathbf{y_{do}} = \bar{\mathbf{C}}\bar{\mathbf{x}} \tag{9}$$

where the matrices $\bar{\mathbf{A}}$, $\bar{\mathbf{B}}$ and $\bar{\mathbf{C}}$ are

$$\bar{\mathbf{A}} = \begin{bmatrix} \mathbf{A} & \mathbf{B}\mathbf{C_{d_i}} & \mathbf{0} \\ \mathbf{0} & \mathbf{A_{d_i}} & \mathbf{0} \\ \mathbf{B_{d_o}}\mathbf{C} & \mathbf{0} & \mathbf{A_{d_o}} \end{bmatrix} \tag{10}$$

$$\bar{\mathbf{B}} = \begin{bmatrix} \mathbf{B}\mathbf{D_{d_i}} & \mathbf{B_{d_i}} & \mathbf{0} \end{bmatrix}^T \tag{11}$$

$$\bar{\mathbf{C}} = \begin{bmatrix} \mathbf{D_{d_o}}\mathbf{C} & \mathbf{0} & \mathbf{C_{d_o}} \end{bmatrix} \tag{12}$$

C. Controlled System

We use the following structure to design a linear dynamic output feedback controller for the power system model (8-9)

$$\dot{\mathbf{x}}_\mathbf{c} = \mathbf{A_c}\mathbf{x_c} + \mathbf{B_c}\mathbf{u_c} \tag{13}$$

$$\mathbf{y_c} = \mathbf{C_c}\mathbf{x_c} + \mathbf{D_c}\mathbf{u_c} \tag{14}$$

where $\mathbf{x_c}$ is the controller state vector, $\mathbf{u_c}$ is the vector of stabilizing signals, $\mathbf{y_c}$ is the vector of controller outputs.

D. Closed Loop System

Using (10-12) to represent the power system with time delays and including the dynamical compensators given by (13-14), the closed loop system can be represented by

$$\begin{bmatrix} \dot{\bar{\mathbf{x}}} \\ \dot{\mathbf{x}}_\mathbf{c} \end{bmatrix} = \begin{bmatrix} \bar{\mathbf{A}} + \bar{\mathbf{B}}\mathbf{D_c}\bar{\mathbf{C}} & \bar{\mathbf{B}}\mathbf{C_c} \\ \mathbf{B_c}\bar{\mathbf{C}} & \mathbf{A_c} \end{bmatrix} \begin{bmatrix} \bar{\mathbf{x}} \\ \mathbf{x_c} \end{bmatrix} \tag{15}$$

Defining the matrices

$$\mathbf{A_a} = \begin{bmatrix} \bar{\mathbf{A}} & \bar{\mathbf{B}}\mathbf{C_c} \\ \mathbf{0} & \mathbf{A_c} \end{bmatrix} \quad \mathbf{B_a} = \begin{bmatrix} \bar{\mathbf{B}} & \mathbf{0} \\ \mathbf{0} & \mathbf{I} \end{bmatrix} \tag{16}$$

$$\mathbf{C_a} = \begin{bmatrix} \bar{\mathbf{C}} & \mathbf{0} \end{bmatrix} \quad \mathbf{G_a} = \begin{bmatrix} -\mathbf{D_c} & -\mathbf{B_c} \end{bmatrix}^T \tag{17}$$

and the augmented state vector $\mathbf{x_a} = \begin{bmatrix} \mathbf{x}^T & \mathbf{x_c}^T \end{bmatrix}^T$, an augmented system can be defined by

$$\dot{\mathbf{x}}_\mathbf{a} = \mathbf{A_a}\mathbf{x_a} + \mathbf{B_a}\mathbf{u_a} \tag{18}$$

$$\mathbf{y_a} = \mathbf{C_a}\mathbf{x_a} \tag{19}$$

and the controlled system given by (15) corresponds to the augmented system given by (18-19) with the output feedback $\mathbf{u_a} = -\mathbf{G_a}\mathbf{y_a}$ or $\mathbf{u_a} = -\mathbf{G_a}\mathbf{C_a}\mathbf{x_a}$. If the canonical observability form is used to represent the controller in (13-14) and if the poles of the controller are fixed, matrices $\mathbf{A_a}$, $\mathbf{B_a}$ and $\mathbf{C_a}$ are known. Matrices $\mathbf{D_c}$ and $\mathbf{B_c}$, corresponding to the gain and zeros of the central controller must be determined from the static output gains. Therefore the dynamic compensator problem is reduced to a constant output feedback problem [3].

III. Centralized Control Design

A. Original Design Method

In [3] is presented a procedure to design a central controller using Linear Quadratic Regular (LQR) and the solution of the Riccati equation. This procedure takes into account on the resulting control strategy the existence of practical structural constraints, such as decentralization and output feedback. Notice that the output feedback constrain is the only relevant one for the two-level control scheme.

The method main goal is to determine a time-invariant feedback gain matrix such that the closed loop system satisfies the power system damping requirements. In order to solve it, a quadratic objective function is minimized (LQR Problem) [19], that is

$$\mathbf{J}(\mathbf{x_a}, \mathbf{u_a}) = \frac{1}{2}\int_0^\infty (\mathbf{x_a}^T\mathbf{Q}\mathbf{x_a} + \mathbf{u_a}^T\mathbf{R}\mathbf{x_a})dt \tag{20}$$

where the positive definite matrix $\mathbf{R}$ and the semi-definite positive matrix $\mathbf{Q}$ are weighting matrices. In [3], $\mathbf{R}$ was chosen as an identity matrix and $\mathbf{Q}$ was chosen as a diagonal matrix with states associated to low damped oscillation modes. The states associated with the low damped modes are strongly weighted.

The solution of the structurally constrained optimal control problem is obtained through the *Generalized Riccati Equation*

$$\mathbf{A_a}^T\mathbf{P} + \mathbf{P}\mathbf{A_a} - \mathbf{P}\mathbf{B_a}\mathbf{R}^{-1}\mathbf{B_a}^T\mathbf{P} + \mathbf{Q} + \mathbf{L}^T\mathbf{R}\mathbf{L} = \mathbf{0} \tag{21}$$

where $\mathbf{L}$ is a matrix which is used to include the structural constraints. Notice that, if the matrix $\mathbf{L}$ is set equal to zero ($\mathbf{L} = \mathbf{0}$) the equation (21) becomes exactly to the original Riccati equation (centralized control and state feedback).

B. Design Method Considering Uncertainties [17]

Consider the system (18-19), the uncertain large-scale interconnected system composed of N uncertain subsystems can be written as [17]

$$\dot{\mathbf{x}}_\mathbf{a} = (\mathbf{A_{a0}} + \mathbf{\Delta A_a})\mathbf{x_a} + (\mathbf{B_{a0}} + \mathbf{\Delta B_a})\mathbf{u_a} \quad (22)$$

$$\dot{\mathbf{x}}_\mathbf{a} = (\mathbf{A_{a0}} + \frac{1}{N}\sum_{j=1}^{N}\mathbf{A_{a}}_j)\mathbf{x_a} + (\mathbf{B_{a0}} + \frac{1}{N}\sum_{j=1}^{N}\mathbf{B_{a}}_j)\mathbf{u_a} \quad (23)$$

where $\mathbf{A_{a0}}$ and $\mathbf{B_{a0}}$ are the nominal operating point and $\mathbf{\Delta A_a}$ and $\mathbf{\Delta B_a}$ represent the uncertainties.

Besides, the uncertainties of the system can satisfy the following matching conditions $\mathbf{\Delta A_a} = \mathbf{B_a G}$ and $\mathbf{\Delta B_a} = \mathbf{B_a H}$ [17]. These uncertainties can be included in the matrices $\mathbf{R}$ and $\mathbf{Q}$ of the original design method [3]. For the uncertainties described in (22) the matrix $\mathbf{R}$ is chosen as [17]

$$\mathbf{R} = \gamma\mathbf{I} = \frac{\beta}{\sigma}\mathbf{I} \quad (24)$$

where

$\sigma = (1 + 2\eta)$ $\quad\quad$ $\eta > 1$ is a real scalar number
$\beta = \min[\lambda_{min}\left(\mathbf{H}^T + \mathbf{H}\right) + \mathbf{I}]$

and

$$\mathbf{Q} \succ \mathbf{G}^T\mathbf{G} + \frac{1}{\eta}\left(1 + \bar{H}^2\right)\mathbf{L}^T\mathbf{L} \quad (25)$$

where

$$\bar{H} = \max||\mathbf{H}|| \quad (26)$$

C. Proposal Procedure

Step 1: Define the order and the poles of the controller and, then, build the matrices $\mathbf{A_c}$ and $\mathbf{C_c}$ in the canonical form;
Step 2: Define the time delays and build the matrices $\mathbf{A_a}$, $\mathbf{B_a}$ and $\mathbf{C_a}$ for all N operating points and define $\epsilon > 0$;
Step 3: Determine $\mathbf{\Delta A_a}$ and $\mathbf{\Delta B_a}$ from the set of N operating points:

$$\mathbf{\Delta A_a} = \frac{1}{N}\sum_{i=1}^{N}\mathbf{A_{a}}_i \quad (27)$$

$$\mathbf{\Delta B_a} = \frac{1}{N}\sum_{i=1}^{N}\mathbf{B_{a}}_i \quad (28)$$

Step 5: Calculate $\mathbf{G} = (|\mathbf{B_a}|^T|\mathbf{B_a}|)^{-1}|\mathbf{B_a}^T||\mathbf{\Delta A_a}|$ and $\mathbf{H} = (|\mathbf{B_a}|^T|\mathbf{B_a}|)^{-1}|\mathbf{B_a}^T||\Delta\mathbf{B_a}|$;
Step 6: Define $\eta > 0$, $r > 0$, $\rho > 0$ and calculate $\mathbf{R}$ as (24) and $\mathbf{Q_0} = r\mathbf{G}^T\mathbf{G} + \rho\mathbf{I}$;
Step 7: Define $k = 0$ and $\mathbf{L_0} = \mathbf{0}$ and solve the Riccati equation $\mathbf{A_a}^T\mathbf{P_0} + \mathbf{P_0 A_a} - \mathbf{P_0 B_a R}^{-1}\mathbf{B_a}^T\mathbf{P_0} + \mathbf{Q_0} = \mathbf{0}$;
Step 8: Set $k = k + 1$ and calculate

$$\mathbf{L}_k = \mathbf{R}^{-1}\mathbf{B_a P}_{k-1}\left[\mathbf{I} - \mathbf{C_a}^T(\mathbf{C_a C_a}^T)^{-1}\mathbf{C_a}\right] \quad (29)$$

$$\mathbf{Q}_k = \mathbf{Q_0} + \frac{1}{\eta}\left(1 + \bar{H}^2\right)\mathbf{L}_k^T\mathbf{L}_k \quad (30)$$

Step 9: Solve the Riccati equation

$$\mathbf{A_a}^T\mathbf{P}_k + \mathbf{P}_k\mathbf{A_a} - \mathbf{P}_k\mathbf{B_a R}^{-1}\mathbf{B_a}^T\mathbf{P}_k + \mathbf{Q}_k = \mathbf{0} \quad (31)$$

Step 10: If $||\mathbf{L}_k - \mathbf{L}_{k-1}||_e < \epsilon$, go to the Step 11, otherwise go to the Step 8;
Step 11: Calculate $\mathbf{K} = \mathbf{R}^{-1}\mathbf{B_a}^T\mathbf{P}_{k-1} - \mathbf{L}_k$ and $\mathbf{G_a} = \mathbf{K C_a}^T(\mathbf{C_a C_a}^T)^{-1}$;
Step 12: Determine $\mathbf{B_c}$ and $\mathbf{D_c}$ through

$$\mathbf{G_a} = \begin{bmatrix} -\mathbf{D_c} & -\mathbf{B_c} \end{bmatrix}^T \quad (32)$$

IV. Application Results

The proposal procedure based on Riccati equation were applied in an IEEE benchmark system for small-signal analysis: the Brazilian 7 bus Equivalent Model [20], shown in the Fig. 1. This power system model presents 5 synchronous generators of fifth-order and the same AVR model with limiters for all generators. A washout filter with a time constant of 10 seconds were used in the inputs of the decentralized and centralized controllers.

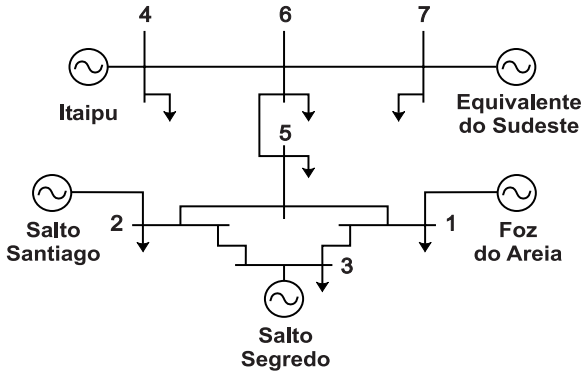

Fig. 1. Brazilian 7 bus Equivalent Model [4], [21].

Table I presents the open-loop system dominant oscillation modes (without any controller) of this power system for an operating nominal condition. As can be seen, there are two inter-area modes.

TABLE I
Open-Loop System Dominant Oscillation Modes

Mode	Eigenvalue	Frequency (Hz)	Damping (%)
1	$0.64 \pm 5.39i$	0.86	-11.9
2	$-0.22 \pm 5.87i$	0.93	3.84

In order to stabilize and improve the system minimum damping, the reference [20] designed four PSSs placed in four generators: Foz do Areia, Salto Santiago, Salto Segredo and Itaipu. Table II, row 1 provides the decentralized control

dominant oscillation modes with these designed PSSs. As can be seen, the damping ratio is higher than 5% (safe condition [22]) for this nominal operating condition.

However, if we consider some contingencies in this nominal operating condition such as a typical daily load variation ($\pm 46\%$ of base load) and topological changes (transmission lines disconnections (1-3) and (2-3)) resulting in 72 different operating conditions, the decentralized control dominant oscillation modes are presented in Table II, row 2. As you can see, the closed loop system with PSSs presents unstable modes of 1.71%. This operating point is -46% of the base case load and without the transmission line (2-3) and will be called the worst case (WC).

TABLE II
DECENTRALIZED CONTROL DOMINANT OSCILLATION MODES

Case	Eigenvalue	Frequency (Hz)	Damping (%)
Base [3]	$-0.33 \pm 5.20i$	0.82	6.39
Worst of 72	$0.09 \pm 4.96i$	0.79	-1.71

Then, we must design a robust central controller, considering the 72 points of operation that were linearized ($\mathbf{A_{a_i}}, \mathbf{i} = 1, ..., \mathbf{N}, \mathbf{N} = 72$), ensuring a minimum damping of 5%. Besides, the central controller must present robustness to time delay variation. To do this, the 72 operating points were considered to obtain the uncertainty matrix $\mathbf{\Delta A_a}$, eq. (27). Estimated time delays of 200 ms were introduced for the two methods at the system inputs and outputs, resulting in a total time delay of 400 ms. However, for the proposed procedure time delays of 100 and 300 ms were also considered to obtain the matrix $\mathbf{\Delta B_a}$, eq. (28).

Two control designs are realized: without operation uncertainties (Not Robust LQR, NR-LQR), using the method presented in [3], and considering system operation uncertainties (Robust LQR, R-LQR), proposed in this paper. The difference between the two methods is the choice of the matrices $\mathbf{R}$ and $\mathbf{Q}$. The designed controllers have 4 inputs (generators speed deviation of the bars 1 to 4) and 4 outputs. The parameters of the procedure were: $\epsilon = 0.02$, $\eta = 200$, $r = 5$ and $\rho = 0.01$. The controller order was 3 and the three poles equal to -10. The resulting central controller are presented in (33).

A. Robustness to Load and Topological Variations

Table III provides the minimum damping modes of the closed loop system with the centralized controllers designed by the two methods for two operating points: the base case (BC) (Table II, row 1) and the worst case (WC) (Table II, row 2) considering a time delay of 200 ms. In [3], a central controller was designed for the nominal operating point and considering a time delay of 200 ms.

Non-linear time-domain simulations were carried out in the power system with the two designed central controllers using ANATEM software [23]. A temporary three-phase short-circuit of 30 ms was applied at bus 4 (Itaipu) and cleared without any switching for the two operating points. The angle and field voltage of the generator 4 (Itaipu) for the base case are presented in the Figs. 2(a) and 2(b), respectively. The angle and field voltage of the generator 4 (Itaipu) for the worst case are presented in the Figs. 2(c) and 2(d), respectively. The R-LQR controller provided better damping in the angle response than the NR-LQR controller for the operating points of Table III.

TABLE III
MINIMUM DAMPING MODES OF THE CLOSED-LOOP SYSTEM WITH WADC

Case	Method	Eigenvalue	Freq. (Hz)	Damping (%)
BC	R-LQR	$-1.71 \pm 13.68i$	2.18	12.45
	NR-LQR	$-0.49 \pm 5.02i$	0.80	9.65
WC	R-LQR	$-0.45 \pm 4.69i$	0.75	9.46
	NR-LQR	$-0.13 \pm 4.82i$	0.77	2.77

B. Robustness to Time Delay Variation

Table IV provides the minimum damping modes of the closed loop system with the centralized controllers designed by the two methods for one operating point: the worst case (WC) (Table II, row 2) considering a time delay (T) of 100 and 300 ms. As you can see, the damping of the closed-loop system is higher than 5%, considered safety [22], when the central controller is designed by the R-LQR method.

TABLE IV
MINIMUM DAMPING MODES OF THE CLOSED-LOOP SYSTEM WITH WADC

T (ms)	Method	Eigenvalue	Freq. (Hz)	Damping (%)
100	R-LQR	$-0.67 \pm 12.16i$	1.93	5.53
	NR-LQR	$0.03 \pm 4.72i$	0.75	-0.55
300	R-LQR	$-0.32 \pm 5.64i$	0.90	5.68
	NR-LQR	$-0.17 \pm 5.15i$	0.82	3.30

Non-linear time-domain simulations were carried out in the power system with the two controllers. A temporary three-phase short-circuit of 30 ms was applied at bus 4 (Itaipu) and cleared without any switching. The angle and field voltage of the generator 4 (Itaipu) for the worst case and T = 100 ms are presented in the Figs. 3(a) and 3(b) respectively, and for T = 300 ms are presented in the Figs. 3(c) and 3(d) respectively. The R-LQR controller provided better damping in the angle response than the NR-LQR controller for time delay variation. The angle and field voltage responses for NR-LQR are unstable when T = 100 ms.

V. CONCLUSIONS

The paper main goal was to propose and apply a procedure based on Riccati equation considering power system operation uncertainties such as load, topological and time delay variations. The controller order is fixed to allow practical applications. The procedure is an improvement of the method presented in [3]. Based on the achieved results, the controller

$$CC(s) = \begin{bmatrix} \frac{19.1s^3+572.6s^2+5726s+19090}{s^3+30s^2+300s+1000} & \frac{39.4s^3+1183s^2+11830s+39420}{s^3+30s^2+300s+1000} & \frac{6.6s^3+132.4s^2+666s+13.08}{s^3+30s^2+300s+1000} & \frac{2.8s^3+85.46s^2+854.7s+2849}{s^3+30s^2+300s+1000} \\ \frac{-5.7s^3-171.1s^2-1711s-5704}{s^3+30s^2+300s+1000} & \frac{-29.5s^3-884.1s^2-8841s-29470}{s^3+30s^2+300s+1000} & \frac{5.9s^3+176.1s^2+1761s+5871}{s^3+30s^2+300s+1000} & \frac{7.6s^3+228.7s^2+2287s+7622}{s^3+30s^2+300s+1000} \\ \frac{-8.0s^3-238.9s^2-2390s-7965}{s^3+30s^2+300s+1000} & \frac{-17.3s^3-520.2s^2-5202s-17340}{s^3+30s^2+300s+1000} & \frac{-17.9s^3-537.4s^2-5374s-17910}{s^3+30s^2+300s+1000} & \frac{20s^3+598.6s^2+5986s+19950}{s^3+30s^2+300s+1000} \\ \frac{-23.3s^3-698.3s^2-6984s-23280}{s^3+30s^2+300s+1000} & \frac{-10.7s^3-320.4s^2-3204s-10680}{s^3+30s^2+300s+1000} & \frac{-10s^3-301.2s^2-3012s-10040}{s^3+30s^2+300s+1000} & \frac{-54.9s^3-1647s^2-16470s-54890}{s^3+30s^2+300s+1000} \end{bmatrix} \tag{33}$$

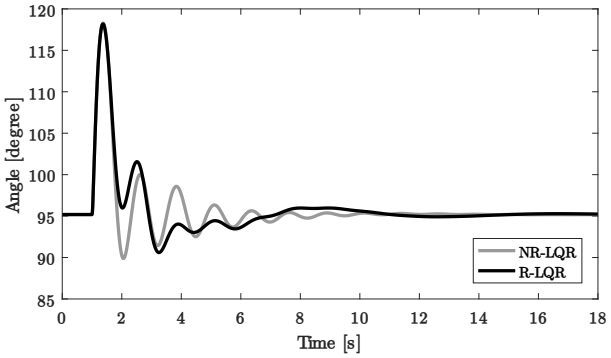

(a) Angle of Itaipu for the base case.

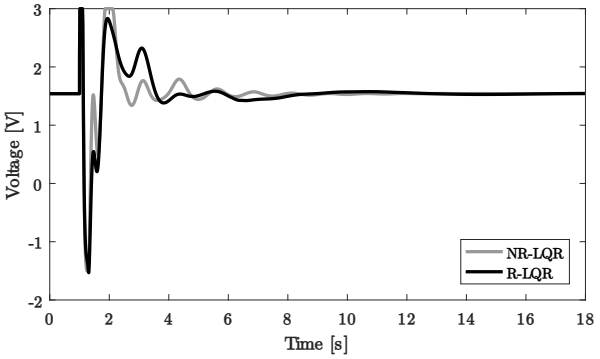

(b) Field voltage of Itaipu for the base case.

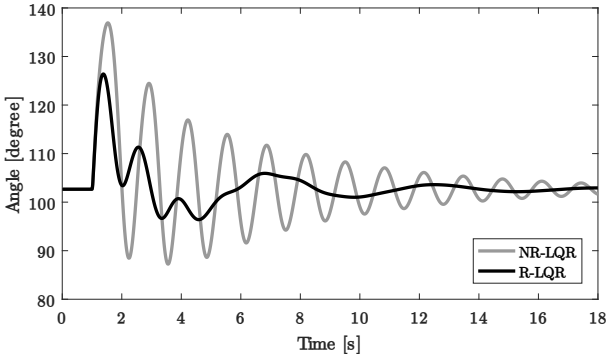

(c) Angle of Itaipu for the operating point of Table III, row 2.

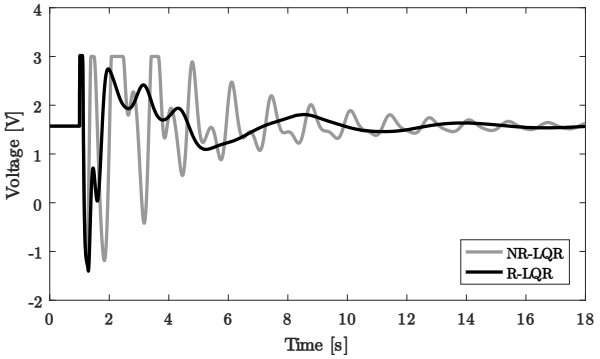

(d) Field voltage of Itaipu for the operating point of Table III, row 2.

Fig. 2. Non-linear simulations with T = 200 ms.

designed by the current proposal procedure provided better performance for operation uncertainties than the original design method. The damping of all modes was significantly improved by the controller designed considering uncertainties.

REFERENCES

[1] P. Kundur, N. J. Balu, and M. G. Lauby, *Power system stability and control*. McGraw-hill New York, 1994, vol. 7.

[2] D. Trudnowski, D. Kosterev, and J. Undrill, "Pdci damping control analysis for the western north american power system," in *2013 IEEE Power Energy Society General Meeting*, July 2013, pp. 1–5.

[3] D. Dotta, A. S. e Silva, and I. C. Decker, "Wide-area measurements-based two-level control design considering signal transmission delay," *IEEE Transactions on Power Systems*, vol. 24, no. 1, pp. 208–216, 2009.

[4] M. E. C. Bento, D. Dotta, and R. A. Ramos, "Performance analysis of Wide-Area Damping Control Design methods," in *2016 IEEE Power and Energy Society General Meeting (PESGM)*. IEEE, jul 2016, pp. 1–5, doi: 10.1109/PESGM.2016.7741334.

[5] Y. Zhang and A. Bose, "Design of wide-area damping controllers for interarea oscillations," *IEEE Transactions on Power Systems*, vol. 23, no. 3, pp. 1136–1143, aug 2008.

[6] V. A. de Campos and J. J. da Cruz, "Robust hierarchized controllers using wide area measurements in power systems," *International Journal of Electrical Power & Energy Systems*, vol. 83, pp. 392–401, dec 2016.

[7] Y. Yuan, Y. Sun, and L. Cheng, "Design of Delayed-Input Wide-area FACTS Controller Using Genetic Algorithm," in *2007 IEEE Power Engineering Society General Meeting*. IEEE, jun 2007, pp. 1–6.

[8] M. E. C. Bento, "Efficiency analysis of local and central controllers in an electric power system," in *2016 12th IEEE International Conference on Industry Applications (INDUSCON)*. IEEE, nov 2016, pp. 1–7.

[9] Shaobu Wang, Yonghui Yi, Zhaoyan Liu, Quanyuan Jiang, and Yijia Cao, "Wide-area damping control reckoning with feedback signals multiple delays," in *2008 IEEE Power and Energy Society General Meeting - Conversion and Delivery of Electrical Energy in the 21st Century*. IEEE, jul 2008, pp. 1–7.

[10] I. Ngamroo, C. S. Ali Nanda, S. Dechanupaprittha, M. Watanabe, and Y. Mitani, "A robust SMES controller design for stabilization of inter-area oscillations based on wide area synchronized phasor measurements," *Electric Power Systems Research*, vol. 79, no. 12, pp. 1738–1749, dec 2009.

[11] C. S. A. Nandar, I. Ngamroo, S. Dechanupaprittha, M. Watanabe, and Y. Mitani, "GPS synchronized phasor measurement units-based wide area robust PSS parameters optimization," *European Transactions on Electrical Power*, vol. 21, no. 1, pp. 345–362, jan 2011.

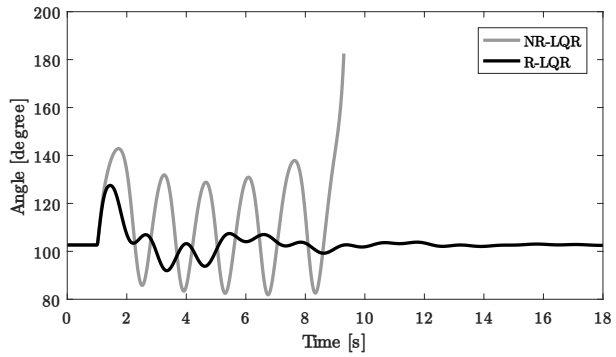

(a) T = 100 ms: angle of Itaipu.

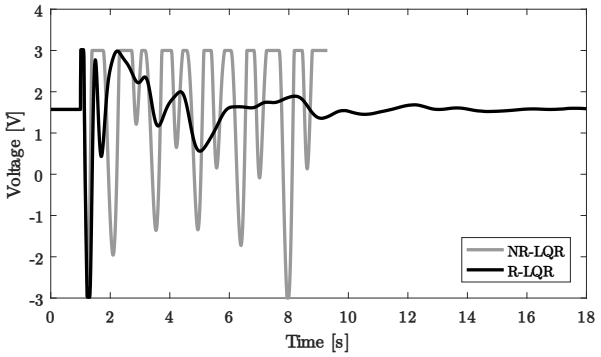

(b) T = 100 ms: field voltage of Itaipu.

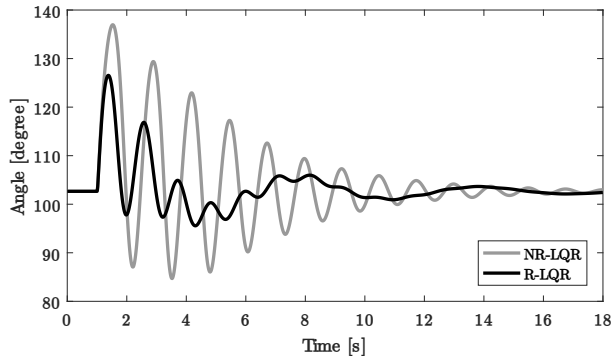

(c) T = 300 ms: angle of Itaipu.

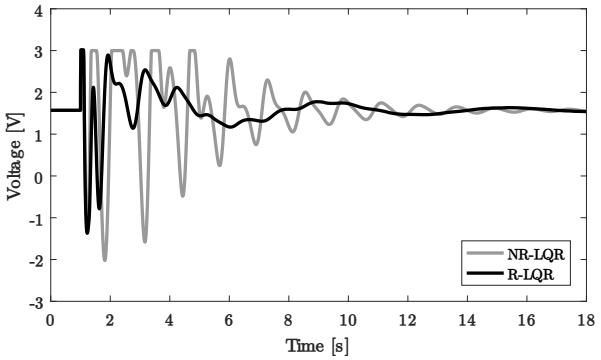

(d) T = 300 ms: field voltage of Itaipu.

Fig. 3. Non-linear simulations.

[12] M. E. C. Bento, "Design analysis of wide-area damping controllers using genetic algorithms," in *2016 12th IEEE International Conference on Industry Applications (INDUSCON)*. IEEE, nov 2016, pp. 1–8.

[13] Min Lu, H. Wu, and X. Li, "Wide area damping control of power systems using particle swarm optimization," in *2009 2nd International Conference on Power Electronics and Intelligent Transportation System (PEITS)*. IEEE, dec 2009, pp. 325–328.

[14] D. Molina, G. K. Venayagamoorthy, and R. G. Harley, "Coordinated design of local and wide-area damping controllers for power systems using particle swarm optimization," in *2013 IEEE Power & Energy Society General Meeting*. IEEE, 2013, pp. 1–5.

[15] M. Mokhtari and F. Aminifar, "Toward wide-area oscillation control through doubly-fed induction generator wind farms," *IEEE Transactions on Power Systems*, vol. 29, no. 6, pp. 2985–2992, nov 2014.

[16] A. M. Annaswamy and M. Amin, "Ieee vision for smart grid controls: 2030 and beyond," *IEEE Vision for Smart Grid Controls: 2030 and Beyond*, pp. 1–168, June 2013.

[17] H. Trinh and M. Aldeen, "Decentralised feedback controllers for uncertain interconnected dynamic systems," *IEE Proceedings D Control Theory and Applications*, vol. 140, no. 6, p. 429, 1993.

[18] M. Vajta, "Some remarks on padé-approximations," in *Proceedings of the 3rd TEMPUS-INTCOM Symposium*, 2000.

[19] J. C. Geromel and P. L. D. Peres, "Decentralised load-frequency control," *IEE Proceedings D Control Theory and Applications*, vol. 132, no. 5, pp. 225–230, 1985, doi: 10.1049/ip-d.1985.0039.

[20] N. Martins and L. T. G. Lima, "Eigenvalue and frequency domain analysis of small-signal electromechanical stability problems," in *Proceedings of the IEEE Symposium on Application of Eigenanalysis and Frequency Domain Method for System Dynamic Performance*, 1989, pp. 17–33.

[21] D. Dotta, "Controle Hierárquico Usando Sinais de Medição Fasorial Sincronizada," Ph.D. dissertation, Universidade Federal de Santa Catarina, Florianópolis-SC, 2009.

[22] S. Gomes, N. Martins, and C. Portela, "Computing small-signal stability boundaries for large-scale power systems," *IEEE Transactions on Power Systems*, vol. 18, no. 2, pp. 747–752, may 2003.

[23] CEPEL, "Anatem user's manual version 10.5.2," 2014, available: http://www.dre.cepel.br/.